Minkovich and Sotsky *Journal of the European Optical Society-Rapid Publications* (2019) 15:7
https://doi.org/10.1186/s41476-019-0103-6

Journal of the European Optical Society-Rapid Publications

RESEARCH Open Access

Tapered photonic crystal fibers coated with ultra-thin films for highly sensitive bio-chemical sensing

Vladimir P. Minkovich[1*] and Alexander B. Sotsky[2]

Abstract

Background: Photonic crystal fiber Mach-Zehnder modal interferometers based on no adiabatic tapered fibers are perspective for bio-chemical sensing, since they have very high refractive index sensitivity and it is possible for them to use a very small quantity of investigated samples. To obtain a desirable sensitivity to a needed analyte, it was proposed to coat a sensing surface of the refractive index sensor with ultra-thin films.

Methods: In this work, we reported on a no adiabatic tapered special photonic crystal fiber coated with an ultra-thin layer of a Bovine Serum Albumin (BSA) antigen or with an 8 nm palladium film to detect interaction between the BSA antigen and an anti-BSA antibody or for fast detection of hydrogen concentrations, respectively.

Results and conclusion: During our experiments, we received a record detection limit of 125 pg/ml of the anti-BSA antibody concentration. Fast detection of hydrogen concentrations up to 5.6 vol% was carried out. By using a proposed electrodynamics model of a hydrogen sensor, an optimal taper sensing length was determined.

Keywords: Optical fiber devices, Optical fiber sensors, Optical fiber interferometer, Photonic crystal fibers

Background

Photonic crystal fiber [1] Mach-Zehnder modal interferometers (PCF MZMIs) based on no adiabatically tapered silica PCFs [2, 3] first were used for a high-resolution refractive index sensing of liquids with indices ranging from 1.33 to 1.45 [2]. It is also known that the PCF MZMIs are temperature-independent up to 180 °C [4]. PCF MZMIs based on no adiabatically tapered fibers are attractive for bio-chemical sensing, because they can have a very small sensing length [2, 3]. To obtain a specific sensitivity for a chosen analyte in a complex composition, it was proposed to coat a sensing surface of a refractive index (RI) sensor with a layer of an active component, characterized with a high affinity to the chosen analyte.

Sensor fabrication and operating mechanism

We employed for fabrication of our tapers a home-made PCF consisting of a solid core surrounded by four rings of air-holes in the cladding arranged in a hexagonal pattern [5]. A micrograph of our PCF cross section is presented in Fig. 1 (left). We used a PCF with the following parameters: outer diameter of 125 μm, core diameter of 11 μm, average hole diameter of 2.7 μm, average hole spacing (pitch) of 5.45 μm. To fabricate a taper, the fiber is heated and stretched. The waist of the PCF (the thinnest part of a taper) are reduced until the air hole collapse [2], obtaining a piece of a solid fiber with the diameter ρ_W ~less than 33 μm. The solid fiber can support multiple modes (waist modes). The beating of these modes inside the solid fiber is sensitive to an external environment. The resulting fundamental mode in the final transition zone (right part of Fig. 1) carries the interference information generated at the tapered zone to the detector. We consider for simplicity only two waist modes for the interference with effective refractive indices, n_1 and n_2. In this case, the taper intensity output is [6]:

$$I_t = I_1 + I_2 + 2\sqrt{I_1 I_2}\cos(\Delta\theta), \quad (1)$$

where I_1 and I_2 are the intensities of the interactive

* Correspondence: vladimir@cio.mx
[1]Centro de Investigaciones en Optica, Division of Photonics, Loma del Bosque 115, Colonia Lomas del Campestre, 37150, Leon, Guanajuato, Mexico
Full list of author information is available at the end of the article

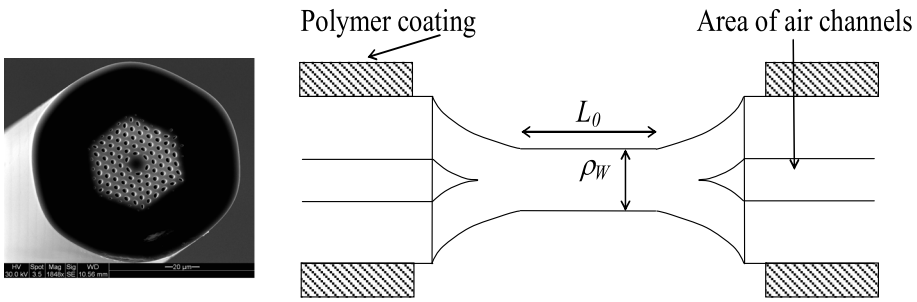

Fig. 1 A micrograph of the PCF cross section (left) and an illustration of the tapered PCF (right). L_0 is the length of the waist and ρ_W is the waist diameter [6]

modes, respectively, and $\Delta\theta$ is the phase difference between them.

This phase difference depends on the difference between the effective mode refractive indices ($\Delta n = n_1$-n_2) and the length of the waist L_0:

$$\Delta\theta = \frac{2\pi}{\lambda}(\Delta n)L_0, \tag{2}$$

where λ is the central wavelength of the light source used. The maxima of the interferometer transmittance will appear at $2\pi\Delta nL_0/\lambda = 2\pi m$, where m is an integer. A change of refractive index of a surrounding medium can be visualized as a shift in the output spectrum pattern [3]. We found that additional losses at tapering of our PCF were typically less than 3 dB.

We implemented for testing of our tapers a setup consisting of an LED with peak emission at 1550 nm (or 1280 nm) and about 80 nm of spectral width and an optical spectrum analyzer (OSA), Ando AQ-6315E. Usually, about 30 cm of the PCF were fusion spliced between standard single-mode fibers (SMF-28). We fabricated a PCF tapered section by heating of a PCF section with an oscillating high-temperature flame torch and slowly stretching it. For PCF tapering, a Vytran GPX3400 also can be used. In all experiments the tapered PCF section was held straight.

Results and discussion

Highly sensitive bio-sensing

For our biosensor experiments, we used a PCF taper with a waist length L_0 = 10 mm and a waist diameter ρ_W = 18.1 μm. To fabricate the taper, we applied a Vytran GPX3400 glass processing machine. The pulling speed at tapering the fiber was kept at 1 mm/s and the heat was arranged at 90 W. An LED source with a center wavelength of 1550 nm and an OSA, Ando AQ-6315E, were used to make the SM-PC-SM fiber transmission spectrum measurements. A special work cell was designed with a working volume of 50 μl and a cavity length of 13 mm to measure small volumes of investigated solutions with our fiber sensor. Before biosensor experiments, we tested a sensitivity of our device for bio-sensing RI range using a sodium chloride (NaCl) diluted in a distilled water in the following concentrations, 0.0, 0.2, 0.4, 0.6, 0.8, and 1 M. Calculated refractive indices of investigated solutions at 1550 are, respectively, 1.30864, 1.31104, 1.31339, 1.31569, 1.31794, and 1.32014 [8]. Figure 2(a) shows that transmission peaks shift to longer wavelength as the refractive indices of the NaCl solutions increase. For the analysis of the peak shifts we selected a peak 1. Correlation of the peak 1 maxima (between 1538 and 1548 nm) with the respective RI of investigated solutions is shown in Fig. 2(b).

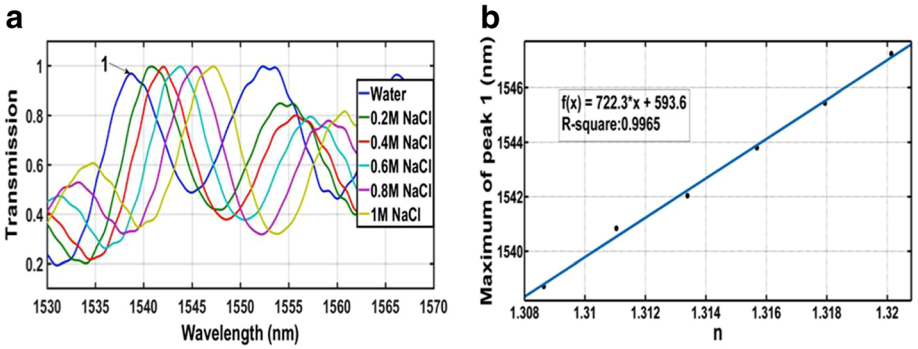

Fig. 2 (**a**)Transmission spectra of the sensor at different concentrations of NaCl, (**b**) linear fit of the sensor response for different concentrations of NaCl with RI between 1.30864 and 1.32014 (reprinted with permission from Ref. [7], IEEE/OSA

It is possible to see that we achieved a sensitivity of 722.3 nm/RIU (with a linearity of 0.9965). Such a sensitivity can be compared with other sensors known. To evaluate the performance of our device for a biosensor application, antigen-antibody tests were carried out. The bovine serum albumin (BSA) antigen was chosen in our experiments. The immobilization process (covalent binding between the BSA antigen and the activated tapered silica surface was conducted like the one presented in [9]. The activation of the taper surface with an aminosilane APTES was carried out preliminary. The biosensor tests were conducted at room temperature (about 25 °C) by using the (anti-BSA) diluted in phosphate-buffered saline (PBS) buffer at different concentrations (125, 12.5, 1.25, and 0.125 ng/ml). We conducted the following procedures. Step 1: Application of the tris (hydroxymethyl) (TRIS) buffer for 3 min to clean the taper surface. Step 2: Removal of the TRIS buffer, application of the PBS, and making a measurement of the optical spectrum that corresponds to the baseline. Step 3: Removal of the PBS buffer, application of the desired anti-BSA solution, and taking measurements for 10 min. We have found in our previous experiments that after about 8 min of interaction the variation of shifts can be neglected. The procedures were repeated for samples with different concentrations of anti-BSA. The difference in a wavelength shift between a baseline peak and the same peak, obtained after 8 min of sample interaction, we related to the sample concentration. The results of our biosensor application, where the magnitude of the response is approximately proportional to the anti-BSA concentration is shown in Fig. 3.

It is possible to see in Fig. 3 that by using our sensor it is possible to measure very low anti-BSA concentrations, with a detection limit of 125 pg/ml, which is lower, for example, than the similar one reported in [10]. Kinetics of BSA antigen-antibody interaction is seen. It is necessary also to point out that our sensor is capable to detect a specific protein inside a complex sample (with different protein solutions). The increased sensitivity in our case is received, since the BSA molecules were immobilized onto the taper surface that has exponentially higher IR sensitivity than areas farther away. The proposed sensor also has a much lower detection limit comparing with those reported in [11, 12], which have detection limits of 10 ng/ml and 1.1 ng/ml, respectively. It was found that the estimated maximum resolution of our sensor was around 1×10^{-2} ng/ml, considering resolution of our spectrum analyzer of 0.05 nm. It is necessary to point out that at using an OSA with a higher resolution an enhanced resolution of our measurements is also possible. For concentrations of anti-BSA between 0.125 and 125 ng/ml we did not have any saturation in a sensor response, see Fig. 3. It is also possible to see in this figure that the spectral shift has highly nonlinear dependence on the anti-BSA concentration. It is necessary to remind that in Fig. 2 we received a linear dependence of our sensor response, when any chemical binding between NaCl solutions and a silica surface was absent. That means, the BSA-antibody binding process has a great impact on our sensor response.

Hydrogen detection

The evanescent fields of PCF propagating waist modes can be changed with different ultra–thin films deposited on a PCF taper. If refractive or absorption indexes of the films are changed under action of external environment, output spectra of a PCF taper will be also changed. In this section the sensing of hydrogen is demonstrated. It is known that hydrogen is explosive in air at a room temperature and pressure at concentrations starting from about 4 vol.% [13]. So, for safety reason it is

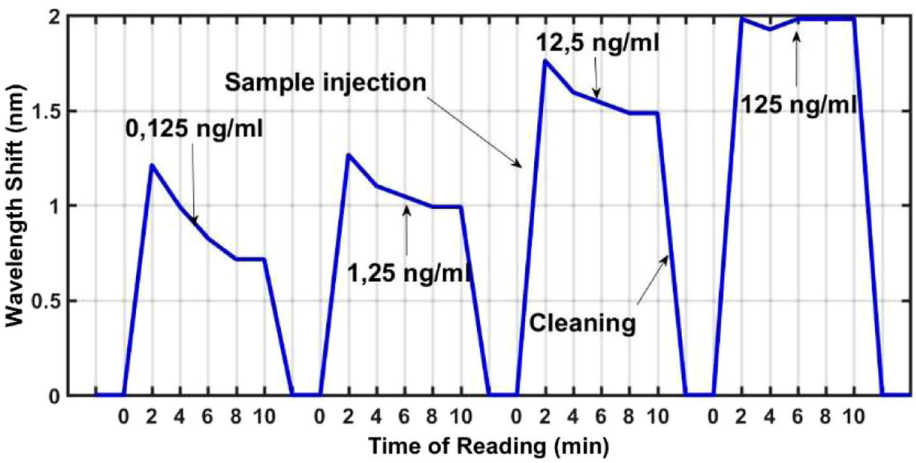

Fig. 3 Sensor response for concentrations of anti-BSA between 0.125 and 125 ng/ml (reprinted with permission from Ref. [7], IEEE/OSA

important a fast detection of hydrogen at low concentrations. It is well known that, when a palladium (Pd) or Pd-alloy film is exposed to hydrogen (H), it is converted to PdH with changing refractive and absorption indexes of a resulting composite material [13–15]. Such changes are possible to monitor at using the developed PCF tapers [6, 16]. For fast detection of low hydrogen concentrations, an eight nanometer palladium film was deposited on the waist of a tapered PCF (with $\rho_W =$ 28 μm) over a length $L_0 = 10$ mm. The film was deposited in a high-vacuum chamber by thermal evaporation. To make the SM-PC-SM fiber transmission spectrum measurements, we used an LED source with a central wavelength of 1280 nm (with 80 nm of spectral width) and an optical spectrum analyzer (OSA), Ando AQ-6315E. Measured transmission spectra of the taper with an 8 nm thick palladium film, which was placed in a nitrogen atmosphere with a hydrogen concentration between 1.2 and 5.6 vol%, are presented in Fig. 4.

It is seen in Fig. 4 that, when the device was exposed to hydrogen concentrations 1.2 to 5.6 vol%, the intensity of the transmitted spectrum peaks increases in a nonlinear manner. The sensor response time was approximately 10 s. Also, a noticeable shift in the output spectrum patterns is absent. It is necessary to point out that at hydrogen concentration more than 6% the transmitted spectrum is similar to that at 5.6%. It means that saturation of the 8 nm thick palladium film takes place. To explain the behavior of the transmission spectra, it was proposed an electrodynamics model accounting for diffraction transformation of local waist modes [17]. Calculation results for the spectral taper transmittance obtained by taking into account $m \geq 9$ local waist modes are presented in Fig. 5.

It is seen in Fig. 5 that an increase of the hydrogen concentration leads to a growth of integral transmittance of the sensor and practically does not affect wavelength positions of transmittance extrema. In such conditions, it is interesting to optimize the sensor from the standpoint of maximizing the sensitivity of its integral transmittance P to a hydrogen concentration C. We investigated possibilities of a sensor optimization by changing the length of the taper waist L_0. Figure 6 shows the calculated normalized sensor transmittance versus C for experimental and optimal L_0 (left) and a sensor sensitivity $(dP/dC)_{C=0}$ versus waist length L_0 (right). It is possible to see in Fig. 6 (left) that the intensity at the output of the sensor is monotonously increasing function of the hydrogen concentration and calculated results are in good accordance with experimental ones (circles). It is possible also to see in Fig. 6 (right) that at $L_0 = 6.375$ mm exists a sensitivity maximum for the investigated sensor. Besides, in the transition from the experimental waist length $L_0 = 10.00$ mm to the optimal value $L_0 = 6.375$ mm, both the transparency and sensitivity of the sensor essentially grow. The existence of a clearly expressed maximum sensitivity of the sensor at $L_0 = 6.375$ mm follows from Fig. 6 (right).

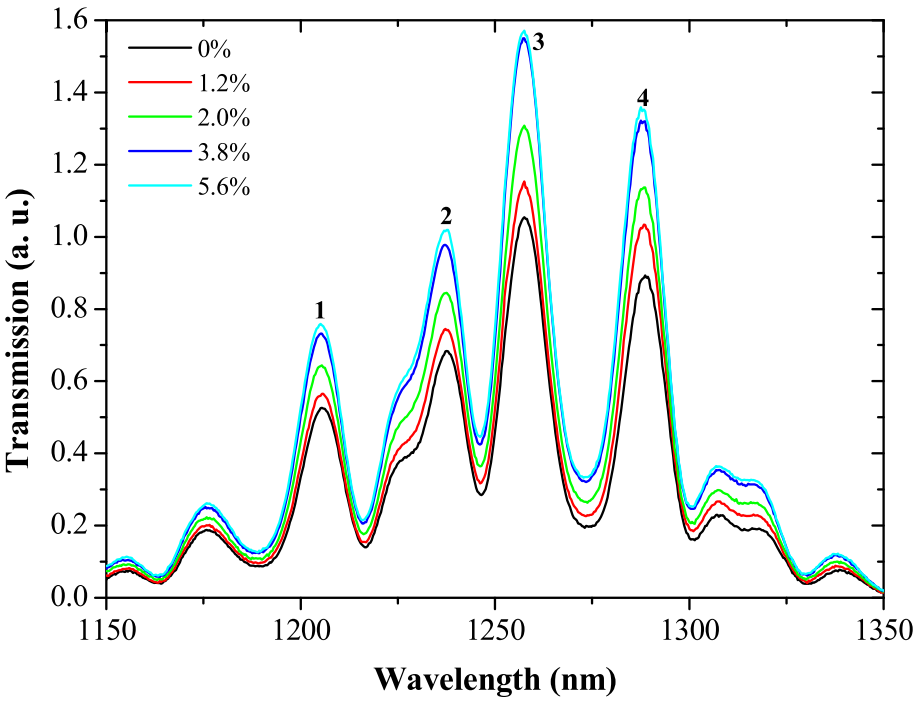

Fig. 4 Transmission spectra of the investigated taper with an 8 nm thick palladium film at different hydrogen concentrations in a nitrogen atmosphere (reprinted with permission from Ref. [16], OSA

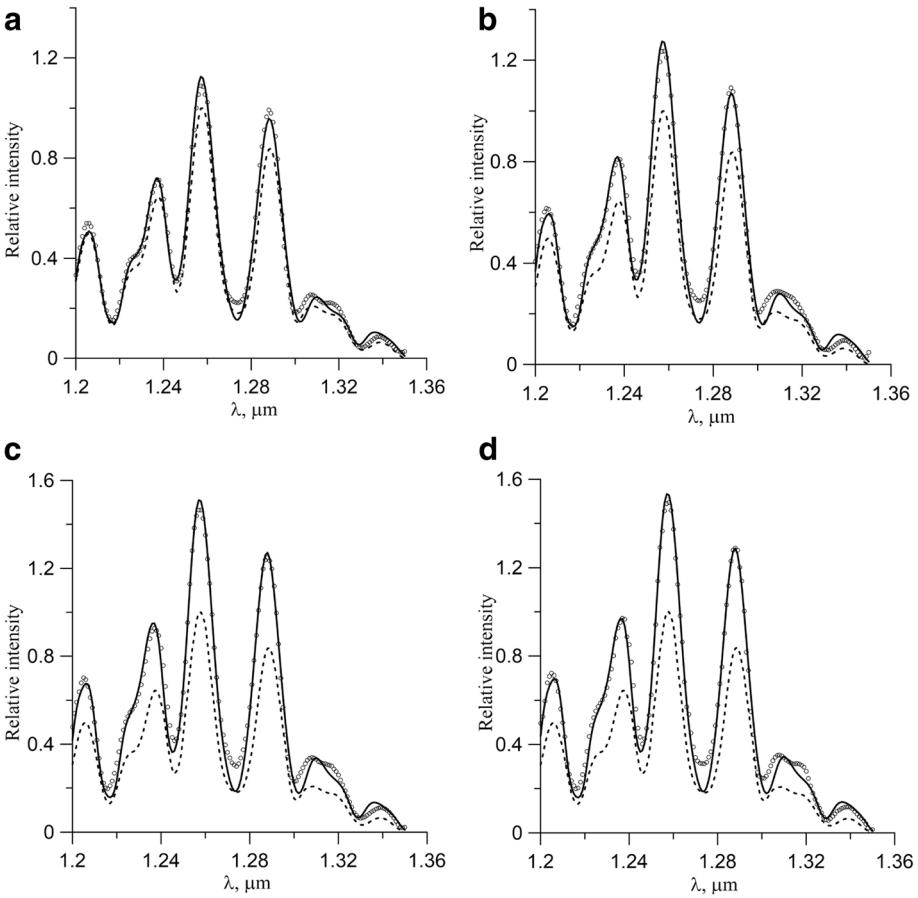

Fig. 5 Calculated results of a relative intensity at the taper output at different hydrogen concentrations (volume %): (**a**) 1.2%, (**b**) 2.0%, (**c**) 3.8%, and (**d**) 5.6% (solid curves); circles are obtained with experiments, dashed lines indicate, for comparison, an interpolation of experimental data at a zero hydrogen concentration

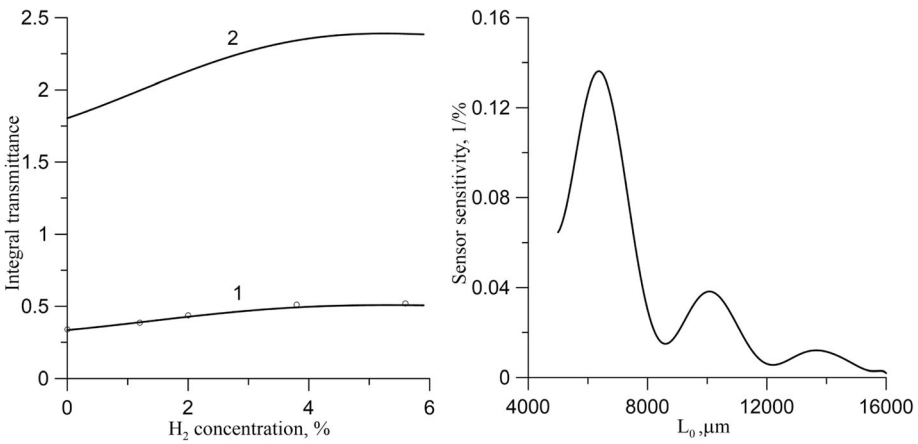

Fig. 6 Calculated integral transmittance of the investigated hydrogen sensor versus a hydrogen concentration (left) and a sensor sensitivity for different waist lengths L_0 (right). Curves 1 and 2 are calculation results for lengths $L_0 = 10.00$ mm and 6.374 mm, respectively. Circles are experimental results

Conclusions

In this paper, we report on compact photonic crystal fiber Mach-Zehnder modal interferometers based on no adiabatically tapered special silica fibers, which were coated with an ultra-thin Bovine Serum Albumin (BSA) antigen or an 8 nm palladium film to detect, respectively, the interaction between the BSA antigen and an anti-BSA antibody with a record detection limit of 125 pg/ml of the antibody concentration or for fast detection of low hydrogen concentrations, between 1.2 and 5.6 vol%. Using a previously developed electrodynamics model, accounting for diffraction transformation of local modes in the taper coated with the 8 nm palladium film, we interpreted obtained experimental data. It was confirmed that an increase of a hydrogen concentration in a nitrogen atmosphere between 1.2 and 5.6 vol% leads to an increase of integral transmittance of the investigated hydrogen sensor and practically does not affect wavelength positions of transmittance maxima. An optimal taper sensing length $L_0 = 6.375$ mm was determined for the investigated hydrogen sensor.

Acknowledgements

Sotsky A.B. would like to thank a Byelorussian State Scientific Program "Photonics 1.3.03" for partially support of this work. The authors also would like to thank their colleagues Villatoro, J., Monzón-Hernandez, D., Kir'yanov, A.V., Calixto, S., Sotskaya, L.I., Badenes, G., Betancur-Ochoa, J.E., and Montagut-Ferizzola, Y.J. for productive scientific cooperation.

Funding

Declared at acknowledgements.

Availability of data and materials

Data sharing is not applicable to this article as no datasets were generated.

Authors´ contributions

Conceived and designed the experiments: VPM, ABS. Performed the experiments: VPM. Analyzed the data: VPM, ABS. Contributed analysis tool: ABS. Wrote the paper: VPM. Both authors read and approved the final manuscript.

Competing interests

The authors declare that they have no competing interests.

Publisher's Note

Author details

[1]Centro de Investigaciones en Optica, Division of Photonics, Loma del Bosque 115, Colonia Lomas del Campestre, 37150, Leon, Guanajuato, Mexico. [2]Dept. of Physics, A.A. Kuleshov Mogilev State University, 1 Kosmonavtov Str, 212009 Mogilev, Belarus.

Received: 28 February 2019 Accepted: 25 April 2019
Published online: 08 May 2019

References

1. Knight, J.C, Birks, T.A, Russell, P.St.J., Atkin, D.M.: All-silica single-mode optical fiber with photonic crystal cladding. Opt. Lett, 21(19),1547–1549(1996), https://doi.org/10.1364/OL.21.001547
2. Minkovich, V.P., Villatoro, J., Monzón-Hernández, D., Calixto, S., Sotsky, A.B., Sotskaya, L.I.: Holey fiber taper with resonance transmission for high-resolution refractive index sensing. Opt. Express. **13**(19), 7609–7614 (2005). https://doi.org/10.1364/OPEX.13.007609
3. Minkovich, V.P., Monzón-Hernández, D., Villatoro, J., Sotsky, A.B., Sotskaya, L.I.: Modeling of holey fiber tapers with selective transmission for sensor applications. J. Lightw. Technol. **24**(11), 4319–4328 (2006). https://doi.org/10.1109/JLT.2006.884207
4. Villatoro, J., Minkovich, V.P., Monzón-Hernández, D.: Temperature-independent strain sensor made of tapered holey optical fibers. Opt. Lett. **31**(3), 305–307 (2006). https://doi.org/10.1364/OL.31.000305
5. Minkovich, V.P., Kir'yanov, A.V., Sotsky, A.B., Sotskaya, L.I.: Large-mode-area holey fibers with a few air channels in cladding: modeling and experimental investigation of modal properties. J. Opt. Soc. Am. B. **21**(6), 1161–1169 (2004). https://doi.org/10.1364/JOSAB.21.001161
6. Minkovich, V.P., Villatoro, J., Sotsky, A.B.: Tapered photonic crystal fibers coated with ultra-thin films for highly sensitive bio-chemical sensing. In: Abstracts of the European Optical Society Biennial Meeting 2018, TU Deft Aula Conference Center, Deft, Netherlands, 8–12 October 2018, 9, 446–447 (2018)
7. Betancur-Ochoa, J.E., Minkovich, V.P., Montagut-Ferizzola, Y.J.: Special photonic crystal modal interferometer for highly sensitive biosensing. J. Lightw. Technol. **35**(21), 4747–4751 (2017). https://doi.org/10.1109/JLT.2017.2761738
8. Li, X., Liu, L., Zhao, J., Tan, J.: Optical properties of sodium chloride solution within the spectral range from 300 to 2500 nm at room temperature. Appl. Spectroscopy. **69**(5), 635–640 (2015). https://doi.org/10.1366/14-07769R
9. Nagel, T., Ehrentreich-Forster, E., Singh, M., Schmitt, K., Brandenburg, A., Berka, A., Bier, F.F.: Direct detection of tuberculosis infection in blood serum using three optical label-free approaches. Sensors Actuators B Chem. **129**(2), 934–940 (2008). https://doi.org/10.1016/j.snb.2007.10.009
10. Yadav, T.K., Narayasnaswamy, R., Abu Bacar, M.H., Mustapha Kamil, Y., Mahdi, M.A.: Single-mode tapered fiber-optic interferometer based refractive index sensor and its application to protein sensing. Opt. Express. **22**(19), 22802–22807 (2014). https://doi.org/10.1364/OE.22.022802
11. Juan Hu, D.J., Lim, J.L., Park, M.K., Kao, L.T.-H., Wang, Y., Wei, H., Tong, W.: Photonic crystal fiber-based interferometric biosensor for streptavidin and biotin detection. IEEE J. Sel. Topics Quantum Electron. **18**(4), 1293–1297 (2012). https://doi.org/10.1109/JSTQE.2011.2169492
12. Yu, W., Lang, T., Bian, J., Kong, W.: Label-free fiber optic biosensor based on thin-core modal interferometer. Sens. Actuators B: Chem. **228**, 322–329 (2016). https://doi.org/10.1016/j.snb.2016.01.029
13. Silva, S.F., Coelho, L., Frazão, O., Santos, J.L., Malcata, F.X.: A review of palladium-based fiber-optic sensors for molecular hydrogen detection. IEEE Sensors J. **12**(1), 93–102 (2012). https://doi.org/10.1109/JSEN.2011.2138130
14. Butler, M.A.: Optical fiber hydrogen sensor. Appl. Phys. Lett. **45**(10), 1007–1009 (1984). https://doi.org/10.1063/1.95060
15. Zhao, Z., Carpenter, M.A., Xia, H., Welsh, D.: All-optical hydrogen sensor based on a high alloy content palladium thin film. Sensors Actuators B Chem. **113**(1), 532–538 (2006). https://doi.org/10.1016/j.snb.2005.03.070
16. Minkovich, V.P., Monzón-Hernández, D., Villatoro, J., Badenes, G.: Microstructured optical fiber coated with thin films for gas and chemical sensing. Opt. Express. **14**(18), 8413–8418 (2006). https://doi.org/10.1364/OE.14.008413
17. Minkovich, V.P., Sotsky, A.B., Shilov, A.V., Sotskaya, L.I.: Taper with palladium coating in photonic crystal fiber as a sensitive element of hydrogen sensor. J. Appl. Spectrosc. Accepted for publication in 2019